Title

Evaluation of aerosol transmission risk during home quarantine under different operating scenarios: A pilot study.

Authors

Cheung, Toby
Li, Jiayu
Goh, Jiamin
et al.

Publication Date

2022-11-01

DOI

10.1016/j.buildenv.2022.109640

Peer reviewed

Since January 2020 Elsevier has created a COVID-19 resource centre with free information in English and Mandarin on the novel coronavirus COVID-19. The COVID-19 resource centre is hosted on Elsevier Connect, the company's public news and information website.

Building and Environment 225 (2022) 109640

Contents lists available at ScienceDirect

Building and Environment

journal homepage: www.elsevier.com/locate/buildenv

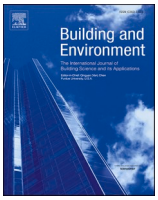

Evaluation of aerosol transmission risk during home quarantine under different operating scenarios: A pilot study

Toby Cheung [a,*], Jiayu Li [b], Jiamin Goh [a], Chandra Sekhar [a], David Cheong [a], Kwok Wai Tham [a]

[a] Department of the Built Environment, National University of Singapore, Singapore
[b] Berkeley Education Alliance for Research in Singapore (BEARS), Singapore

ARTICLE INFO

Keywords:
Aerosol transmission risk
Air conditioning
Natural ventilation
Fans
COVID-19
Home quarantine

ABSTRACT

SARS-CoV-2 has been recognized to be airborne transmissible. With the large number of reported positive cases in the community, home quarantine is recommended for the infectors who are not severely ill. However, the risks of household aerosol transmission associated with the quarantine room operating methods are under-explored. We used tracer gas technique to simulate the exhaled virus laden aerosols from a patient under home quarantine situation inside a residential testbed. The Sulphur hexafluoride (SF_6) concentration was measured both inside and outside the quarantine room under different operating settings including, air-conditioning and natural ventilation, presence of an exhaust fan, and the air movement generated by ceiling or pedestal fan. We calculated the outside-to-inside SF_6 concentration to indicate potential exposure of occupants in the same household. In-room concentration with air-conditioning was 4 times higher than in natural ventilation settings. Exhaust fan operation substantially reduced in-room SF_6 concentration and leakage rate in most of the ventilation scenarios, except for natural ventilation setting with ceiling fan. The exception is attributable to the different airflow patterns between ceiling fan (recirculates air vertically) and pedestal fan (moves air horizontally). These airflow variations also led to differences in SF_6 concentration at two sampling heights (0.1 m and 1.7 m) and SF_6 leakage rates when the quarantine room door was opened momentarily. Use of natural ventilation rather than air-conditioning, and operating exhaust fan when using air-conditioning are recommended to lower exposure risk for home quarantine. A more holistic experiment will be conducted to address the limitations reflected in this study.

1. Introduction

After two and a half years since the outbreak of the Coronavirus disease 2019 (COVID-19), substantial evidence had shown that the severe acute respiratory syndrome coronavirus 2 (SARS-CoV-2), which is the virus that causes COVID-19, is becoming milder in terms of hospitalization demand and deaths [1–5]. Hence, many governments and authorities started recommending that infected people with non-severe symptoms be self-isolated at home to conserve and deploy medical resources for those more seriously ill who urgently need them [6–8]. Infected persons shed viruses across the entire spectrum of oral activities including breathing, talking and singing [9]. However, even though the infected person is recommended to stay in a relatively separate room during the self-quarantine period, emitted airborne viruses escaping to other spaces in the house are often inevitable because residential facilities are not designed for quarantine purpose. Some researchers pointed out that the value of home isolation for COVID-19 patients is relatively low [10], and they suggested all the infected people, even with mild symptoms, should be quarantined in hospitals or *Fangcang shelter* hospitals [11,12]. Moreover, though the newer variants of the SARS-CoV-2, like the Omicron strain, are milder than earlier variants, including the Delta variant, those newer variants are more transmissible [4,13–15] This suggests that it only needs a relatively small amount of the virus leakage from the quarantine room to potentially infect those living in the same house. Hence, to address the debate on the home isolation strategy for mild COVID-19 patients, evaluation of the intra-house transmission risk during the home quarantine period is essential.

During the home quarantine period, the intra-house transmission of the aerosols in a residential house is mainly from the leakages through the cracks between the door and its frame and some necessary door-opening activities of the occupants, such as food delivery and trash removal. The impact of the door-opening activity on the aerosol

* Corresponding author.
E-mail address: toby_bdg@nus.edu.sg (T. Cheung).

https://doi.org/10.1016/j.buildenv.2022.109640
Received 1 August 2022; Received in revised form 22 September 2022; Accepted 24 September 2022
Available online 29 September 2022

transmission between rooms is relatively well studied in healthcare facilities. Using small-scale water-tank models, a study quantitatively evaluated the impact of the door type on containment failures in hospital isolation rooms [16], and another study calculated air exchange and infection transfer between rooms due to door motion [17]. Using three-dimensional ultrasonic anemometers, a study compared the airflow on doorway under different mechanical ventilation strategies, which showed that the door-opening activity can lead to air exchanging between the operating room and the adjacent areas in all ventilation strategies [18]. Similar studies have been conducted in pressurized clean rooms [19] and isolation rooms for nuclear plants [20]. However, there is no reported study focusing the impact of the door opening on aerosol transmission in a residential facility. Moreover, compared to those specially designed doors in healthcare and cleanroom settings, the doors in residential buildings are normally not well sealed, which also allow the emitted viruses in the quarantine room to be leaked out even when the door is closed. It is necessary to explore the transmission risk of the pathogen from the quarantine room to other spaces in a household.

The operating strategy of the isolation room plays a very important role in terms of the airborne pollutant transmission across the door [18]. The operating conditions are dominated by the settings of the air conditioning (AC), the fan, and the window operating status [21]. An opened window enhances air exchange rate with the outdoor air [21,22] which dilutes the emitted pathogen in the isolation room more effectively. Further, the World Health Organization recommended putting a pedestal fan near an open window to enhance the room ventilation [23]. However, those recommended measures only target reducing the aerosol concentration within the quarantine room where other non-infected family members are advised not to enter. Airborne transmission across the door to other spaces within the house remains unknown.

Several studies assume that exhalation from an infected person under quarantine contains the SARS-CoV-2 virus remains airborne, mixes with the air currents within the quarantine room, and follows leakages out of the room. Specifically, the concentration within and outside the room (across the door) are indicative of the potential exposure of household members. Based on those assumptions, both numerical simulations and experimental measurements can be used to evaluate the transmission risk [24]. Although numerical simulations, represented by computational fluid dynamics (CFD) modeling, are more affordable and efficient than physically conducting experiments, the measured experimental results are still valuable and are necessity to validate the CFD models [25,26]. For experiment measurements, considering the reliability and repeatability, the tracer gas methods are widely used to experimentally study the pathogen airborne transmission risk [27,28]. Various tracer gases, such as CO_2 [29,30], SF_6 [31–34], N_2O [35], and Ethane [36] can be used as the surrogates of small respiratory aerosols (<5 μm), and among those, SF_6 is the most often used due to its detectability at low concentrations, low toxicity, and scarcity in the background environment.

In this study, we aim to evaluate the intra-house transmission risk during the COVID-19 home recovery program via the tracer gas method in a residential testbed. We sought to 1) compare the common operating scenarios in the residential room, and 2) evaluate the currently recommended measures for homes prior to lowering the transmission risk.

2. Experimental site

This study was conducted in the Smart Green Home [37], an indoor test-bed in the National University of Singapore to study on smart features and sustainable technologies for residential premises. Our experiment was set up in the master-bedroom of this smart facility to mockup a quarantine room for COVID-19 positive patients serving stay home recovery. Fig. 1a presents a snapshot and Fig. 1b shows a plan view sketch of the quarantine room illustrating the experimental setups. The master-bedroom is 3.2 m (W) x 3.6 m (L) x 3 m (H) in size. An individual toilet approximately 3 m^2 is attached to the test room. Two operable windows, 1 m^2 each, are shown in Fig. 1a, while the remaining larger glazing on the left most is always kept shut. Other openings that allow air exchange were the door gaps, both to the toilet and the living room, each 100 cm (W) x 1.3 cm (H) in size. In addition, the toilet window was opened throughout all tested scenarios.

The test room was installed with a split-type air-conditioning unit (rated capacity 1.5 kW) and a 52-inch ceiling fan (Big Ass Fan, Haiku-I-Series). Both the air-conditioner and ceiling fan are installed ~265 cm above floor. The ceiling fan is located 170 cm from the door and 85 cm from the nearest wall. To facilitate alternative operating strategies, a 16-inch pedestal fan and a 12-inch desk fan were also introduced into the test room. The pedestal fan was fixed at a position 185 cm from the door, 30 cm from the wall, elevated 120 cm above the floor, tilted at an angle 15° above horizontal, and blew the air towards the bed. The desk fan was functioning as a window exhaust in this study, which was positioned 15 cm from the window, elevated 140 cm above the floor, tilted at 20° angle from horizontal, and moved air from the room outside the window.

The Smart Green Home is constructed "within" a building enclosure. Fig. 1a shows the external wall of the test room is recessed ~6 m from the boundary of the building. In addition, the window of the attached toilet is connected to a circulation corridor in the middle of the building. We assume cross ventilation is still feasible when the room windows are opened, but the impacts from outdoor wind condition would be reduced under this site configuration.

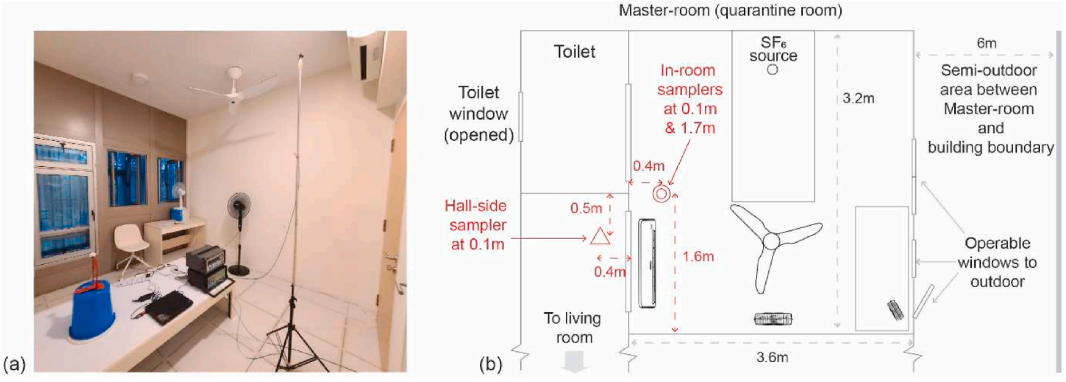

Fig. 1. (a) A snapshot of the master-bedroom; (b) a plan view diagram identifying the experimental setups both inside and outside the master-bedroom (i.e., the quarantine room). Information about in-room and hall-side samplers is highlighted in red. (For interpretation of the references to colour in this figure legend, the reader is referred to the Web version of this article.)

2.1. Operating scenarios and setup

A total of five operating scenarios were tested in our study, including air-conditioning without fan (AC_{only}), air-conditioning with ceiling fan ($AC_{C\text{-}fan}$), air-conditioning with pedestal fan ($AC_{P\text{-}fan}$), natural ventilation with ceiling fan ($NV_{C\text{-}fan}$), and natural ventilation with pedestal fan ($NV_{P\text{-}fan}$). It is noted that the room condition for natural ventilation without any fan is not being considered in our study, because this scenario results in thermal discomfort and is uncommon due to the hot and humid weather in Singapore. Under AC scenarios, the air-conditioner was operated at 25 °C set-point with all windows and doors closed, while the windows and toilet door were fully opened in the two NV scenarios. The door to the living room was closed throughout the experiment, except for the designated door opening procedure which simulates the periodic.

The ceiling fan has a total of 7 speed levels. In both AC and NV settings, the ceiling fan was operated at the same speed level 3 (i.e., 96 rpm and 0.94 m/s measured directly under fan) which has been tested to be thermally comfortable between 24 and 27 °C in a previous study [38]. The pedestal fan has 3 speed levels, and the middle level (i.e., 260 L/s) was chosen for both AC and NV settings. It is noted that the oscillating function of the pedestal fan was disabled in our study to provide a more consistent airflow pattern. The desk fan was used as an exhaust fan dragging air outside the quarantine room at an airflow rate of 170 L/s. The exhaust fan on and off status were both applied to all five testing scenarios in our study. The location and speed for all fans remain unchanged throughout the experiment in the corresponding scenario.

2.2. Physical measurement

We used tracer gas technique to simulate the transmission of exhaled virus-laden droplets from the infected person under quarantine in this study. Sulphur hexafluoride (SF_6) was selected as the tracer gas source and continuously released at a constant dosing rate of 0.1 L/min inside the quarantine room on the bed (see Fig. 1). This optimal dosing rate was selected based on multiple pre-experiments, which the chosen rate of SF_6 release achieved concentration levels that are detectable under all five operating scenarios yet without excessive wastage. The gas releasing tube was attached to a ping-pong ball with multiple holes on its surface, thus SF_6 was distributed uniformly in all directions.

The SF_6 concentration ($SF_{6,conc}$) from three sampling points was measured through an INNOVA 1309 multi-channel sampler with a detection limit of 0.01 ppm and an accuracy ±2 % of the measured value. Two of the sampling probes were fixed inside the room at 0.1 m and 1.7 m heights and located at a distance 0.5 m away from the middle of two doors (see Fig. 1b). The remaining sampling probe was placed at 0.1 m height and located 0.4 m away from the door in the hall-side (i.e., outside the quarantine room). The in-room and hall-side sampling probes at 0.1 m were selected to determine the SF_6 leakage rate via door gap, while the sampler at 1.7 m (i.e., the breathing height of a human subject) was to verify if a vertical stratification of $SF_{6,conc}$ has been developed. Sampling frequency for three sampling points were measured approximately 2 min.

2.3. Experimental procedures

Fig. 2 summarizes the experimental procedures in terms of room settings and actions being taken over the experiment timeline. Five operating scenarios were introduced in our experiment to evaluate virus transmission risk between the quarantine and the living rooms, including AC_{only}, $AC_{C\text{-}fan}$, $AC_{P\text{-}fan}$, $NV_{C\text{-}fan}$, and $NV_{P\text{-}fan}$. All settings associated with these scenarios were prepared inside the quarantine room before the sampling took place. The INNOVA starts sampling 30 min before tracer gas has been released into the quarantine room to establish that the $SF_{6,conc}$ in the background environment was negligible. The full-scale experiment was divided into two phases. In the first phase (without operation of exhaust fan), tracer gas was continuously released at a dosing rate of 0.1 L/s for 180 min. The first 90 min facilitated SF_6 to attain a stable level inside the quarantine room, and the next 90 min was taken to be the steady state condition providing representative $SF_{6,conc}$ for each operating scenario. The assumption of steady state concentration in the latter 90 min was estimated by multiple pre-tests under different room operating settings at the given tracer gas dosing rate (i.e., 0.1 L/s). In the middle of the first phase experiment, we opened the quarantine room door for 10 s to simulate a food delivery/trash cleaning activity. The second phase experiment started right after the first phase, and it began with switching on the window exhaust fan. Similarly, the second phase experiment is a duplicate of the first except that the exhaust fan is now operated. It consisted of 180 min, with the first 90 min attaining stable in-room $SF_{6,conc}$ with operation of exhaust fan, while the next 90 min were taken to be steady state for further $SF_{6,conc}$ analysis. Also, the room door was opened for 10 s in the middle of the second phase experiment. The experiment ended with tracer gas cut-off after the second phase procedures.

2.4. Statistical analysis

We used Null Hypothesis Significance Testing (NHST) [39] to evaluate the differences in $SF_{6,conc}$ collected over the five operating scenarios with/without exhaust fan during the steady state period (i.e., the $SF_{6,conc}$ collected at latter 90 min for both phases of experiment in Fig. 2). The analyses rely on NHST depend on both the sample size and magnitude of the effect. We used two non-parametric statistical tests to analyse the differences in $SF_{6,conc}$ between two ventilation scenarios (i) the Wilcoxon rank-sum test (i.e., *U* test): and (ii) the Cliff's Delta. *U* test is used to compare whether the two samples' population mean rank differ [40]. A *p-value* ≤ 0.05 denotes the threshold of statistical significance for null hypothesis (no difference) being rejected and alternative hypothesis is accepted. The Cliff's Delta statistic is an effect size measure that is used to quantify the difference between two populations beyond *p-value* interpretation [41]. The outcomes of the effect size are interpreted by the absolute |d|-*value* including negligible ($|d| < 0.147$), small ($0.147 \leq$

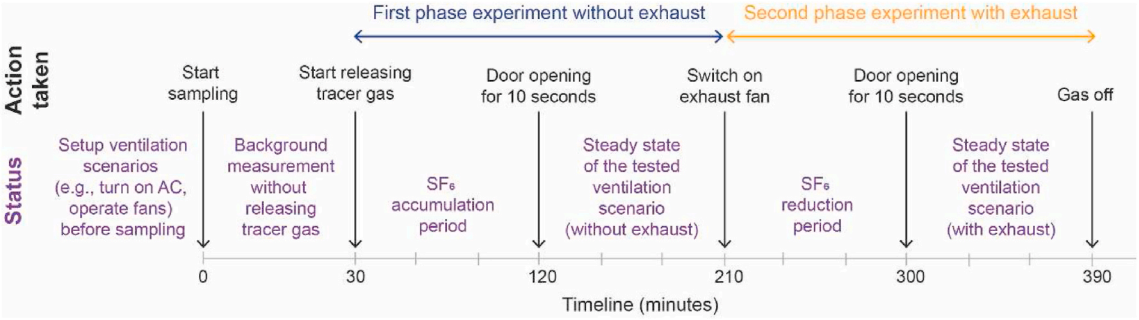

Fig. 2. Detailed indication of experimental procedures for actions being taken, status of the test room, and exhaust fan operation schedule.

|d| < 0.33), medium (0.33 ≤ |d| < 0.474), and large (0.474 ≤ |d|) [42,43]. To maintain consistency, we presented the mean and standard deviation values as a reference indicating the steady state $SF_{6,conc}$ over different operating scenarios despite a non-normal distribution being observed in some cases. All analyses were conducted using R version 4.2.1 [44]. We used the in-built "wilcox.test" function and the "cliff.delta" function in "effsize" package [45] to calculate evaluate the *p-value* and |d|-*value* in this study.

3. Results and discussion

3.1. Time series SF_6 concentration overview

Fig. 3 summarizes the time series Sulphur hexafluoride concentration ($SF_{6,conc}$) data for the three sampling locations (i.e., hall-side 0.1 m height and in-room at both 0.1 m and 1.7 m height) measured under five different operating scenarios (i.e., AC_{only}, $AC_{P\text{-}fan}$, $AC_{C\text{-}fan}$, $NV_{P\text{-}fan}$, and $NV_{C\text{-}fan}$) with both window exhaust fan On and Off conditions. The $SF_{6,conc}$ pattern in all scenarios can be generally broken down into three stages. First, the $SF_{6,conc}$ started to accumulate when tracer gas was emitted in the quarantine room. Meanwhile, tracer gas started to leak outside of the quarantine room, leading to a rise in the hall-side $SF_{6,conc}$. Second, when the exhaust fan was turned on, the $SF_{6,conc}$ reduced and gradually stabilised for both in-room and hall-side sampling points. Lastly, the $SF_{6,conc}$ from all sampling locations reduced to zero after the cut-off of the emission source. On the other hand, a rapid increase in $SF_{6,conc}$ was detected at the hall-side sampling point whenever the door was opened. Throughout these stages, the $SF_{6,conc}$ captured at the three sampling locations with different fan types are discussed and compared among four conditions: Operating strategy (AC vs NV) and Exhaust fan status (Off/On).

3.2. Comparisons by SF_6 concentration

3.2.1. AC scenarios without exhaust fan

All three scenarios (i.e., no fan, pedestal, and ceiling fan) tested under AC condition took approximately 90 min for the $SF_{6,conc}$, at different sampling points to attain a relatively steady level. Assuming in the later 90 min (i.e., from 90 to 180 min in Fig. 3, excluding the door opening outliers) as a steady concentration period, Fig. 4 summarizes the distributions of $SF_{6,conc}$ for all sampling locations and operating scenarios when exhaust fan is turned off (this refers to the duration denoted by the blue arrow in Fig. 3).

Table 1 summarizes the mean and standard deviation (in bracket) for $SF_{6,conc}$ at 0.1 m in-room, 1.7 m in-room, and 0.1 m hall-side. Inside the quarantine room, at both 0.1 m and 1.7 m sampling height, the highest $SF_{6,conc}$ was found at $AC_{P\text{-}fan}$ case, followed by $AC_{C\text{-}fan}$, while the AC_{only} cases has the lowest concentration ($p \leq 0.05$, U test; $|d| \geq 0.474$, large effect size). Meanwhile, we observed higher $SF_{6,conc}$ at 1.7 m than at 0.1 m height for AC_{only} and $AC_{C\text{-}fan}$ cases ($p \leq 0.05$, U test; $|d| \geq 0.474$, large effect size), but the same observation was not found in $AC_{P\text{-}fan}$ setting. The hall-side $SF_{6,conc}$ was not significantly different between AC_{only} and $AC_{C\text{-}fan}$ conditions ($p > 0.05$, U test), but a slightly higher concentration reported in $AC_{P\text{-}fan}$ case ($p \leq 0.05$, U test) with a medium effect size ($|d| \leq 0.33$).

We suspect that the air flow patterns created by the fans are the causes of the above observations. Fig. 5 visualizes the plan view of airflow patterns generated by the (a) pedestal fan and (b) ceiling fan in our experiment. Pedestal fan moves the air horizontally from the bed end directly towards the tracer gas source, which disperses the $SF_{6,conc}$ more effectively within the quarantine room. Thereafter, these air with higher $SF_{6,conc}$ further move towards the wall then rebound back to the door side, and directly captured by the in-room samplers. This explains higher $SF_{6,conc}$ observed in both in-room and hall-side samplers and minimizes the concentration difference between 0.1 m and 1.7 m height

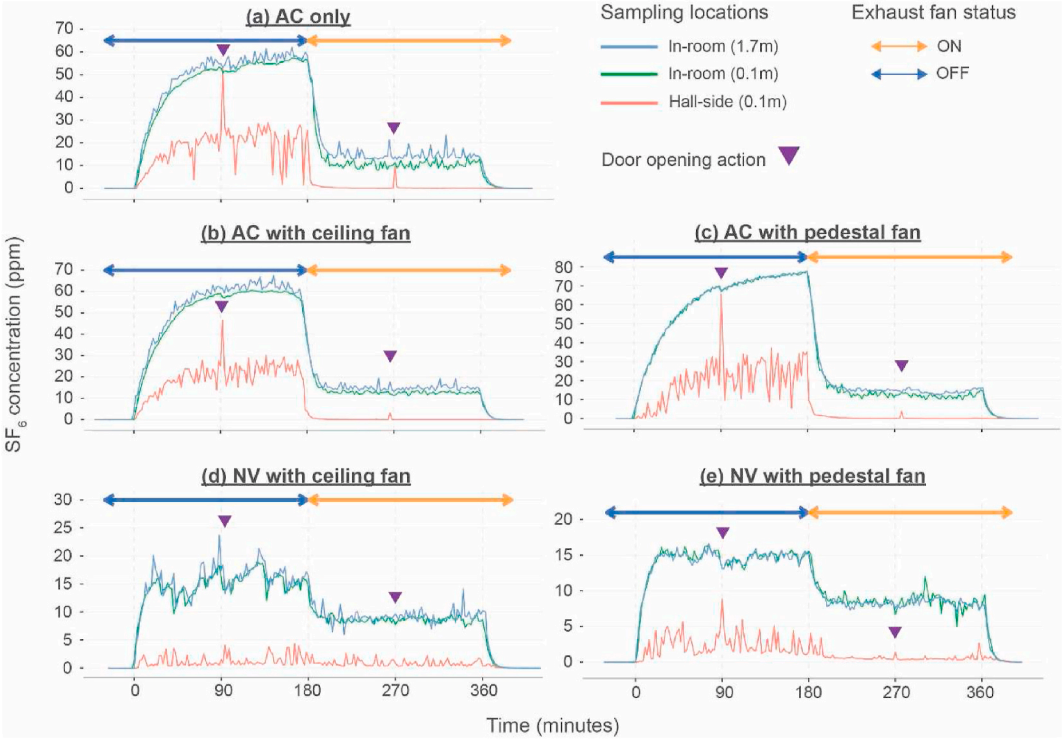

Fig. 3. Time series $SF_{6,conc}$ under different ventilation scenarios with/without window exhaust. (a) Air-conditioning (AC) only, (b) AC with ceiling fan, (c) AC with pedestal fan, (d) Natural ventilation (NV) with ceiling fan, and (e) NV with pedestal fan. The three sampling locations are: hall-side at 0.1 m height (red line), in-room at 0.1 m height (green line), and in-room at 1.7 m height (blue line). (For interpretation of the references to colour in this figure legend, the reader is referred to the Web version of this article.)

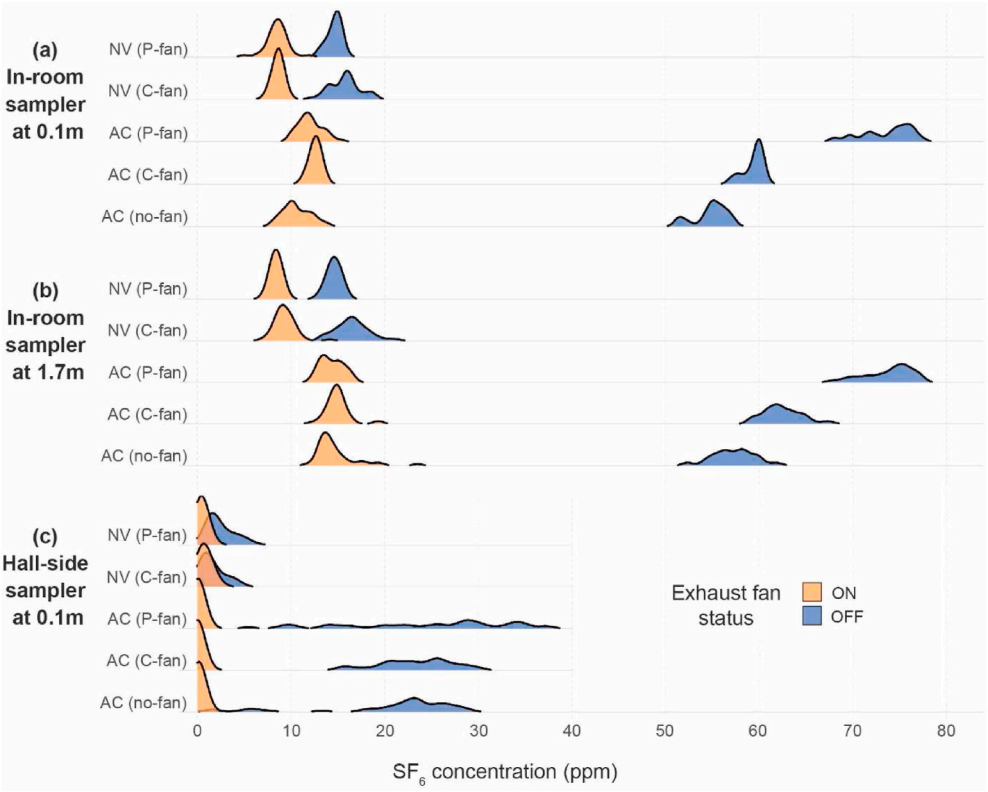

Fig. 4. $SF_{6,conc}$ distribution comparison for window exhaust On and Off status at: (a) In-room sampler at 0.1 m, (b) In-room sampler at 1.7 m and (c) Hall-side sampler at 0.1 m height.

Table 1
Measured mean (standard deviation) of SF_6 concentration at different locations and conditions.

Locations Conditions		0.1 m hall-side (ppm)	1.7 m in room (ppm)	0.1 m hall-side (ppm)
AC without exhaust fan	AC_{only}	54.8 (1.7)	57.3 (2.2)	20.8 (7.3)
	$AC_{P\text{-}fan}$	73.6 (2.7)	73.8 (2.6)	24.5 (8.7)
	$AC_{C\text{-}fan}$	59.4 (1.0)	62.5 (2.2)	23.3 (3.9)
AC with exhaust fan	AC_{only}	10.6 (1.5)	14.7 (2.2)	0.2 (0)
	$AC_{P\text{-}fan}$	12.0 (1.3)	14.4 (1.2)	0.1 (0.1)
	$AC_{C\text{-}fan}$	12.6 (0.6)	15.0 (1.3)	0 (0)
NV without exhaust fan	$NV_{P\text{-}fan}$	14.6 (0.7)	14.6 (0.7)	2.4 (1.3)
	$NV_{C\text{-}fan}$	15.8 (1.6)	16.5 (1.4)	1.6 (1.2)
NV with exhaust fan	$NV_{P\text{-}fan}$	8.6 (1.1)	8.4 (0.5)	0.5 (0.2)
	$NV_{C\text{-}fan}$	8.6 (0.5)	9.4 (1.2)	0.8 (0.5)

in $AC_{P\text{-}fan}$ scenario. Higher $SF_{6,conc}$ at 1.7 m height found in $AC_{C\text{-}fan}$ and AC_{only} scenarios are possibly due to continuous air exchange, i.e., infiltrates in or leaks out, through the door gap, which dilutes the concentration near the floor level. Meanwhile, the operation of ceiling fan enhances air movement, as well air mixing, resulting in higher $SF_{6,conc}$ when compared to AC_{only} scenario.

3.2.2. AC scenarios with exhaust fan

After the exhaust fan was switched on, the $SF_{6,conc}$ dropped substantially in all three AC testing conditions at both in-room (reduced by ~80 %) and hall-side (reduced by ~100 %) samplers. Fig. 4 summarizes the distribution of $SF_{6,conc}$ for different operating scenarios when exhaust fan is switched on (denoted by the duration under the orange arrow in Fig. 3). The mean (standard deviation) $SF_{6,conc}$ at 0.1 m in-room, 1.7 m in-room, and 0.1 m hall-side are summarized in Table 1.

We observed lower $SF_{6,conc}$ at 0.1 m than at 1.7 m height inside the quarantine room for all fan types ($p \leq 0.05$, U test; $|d| \geq 0.474$, large effect size), especially for AC_{only} condition (28 % lower at 0.1 m). These findings are explained by the forced airflow from the window exhaust fan (see Fig. 5c). When the exhaust fan is turned on, it drives air to the outdoors through the window creating a negative pressure in the room. Air is forced to flow into the quarantine room continuously from the toilet and hall-side via the door gaps diluting the $SF_{6,conc}$ at floor level. Regarding fan types, we found no difference in $SF_{6,conc}$, at both 0.1 m and 1.7 m, between $AC_{C\text{-}fan}$ and $AC_{P\text{-}fan}$ scenarios ($p > 0.05$, U test; $|d| < 0.33$, small effect). However, a lower concentration was found in AC_{only} scenario ($p \leq 0.05$, U test) at 0.1 m ($|d| \geq 0.474$, large effect) and at 1.7 m ($|d| < 0.33$, small effect) when compared to the scenarios operating with fans. Plausibly operating fans in $AC_{C\text{-}fan}$ and $AC_{P\text{-}fan}$ scenarios enhance $SF_{6,conc}$ mixing inside the quarantine room compensating the dilution attributable to inflow of air from the hall-side via the door gaps.

The $SF_{6,conc}$ at hall-side were all reported (close to) zero for the three AC test conditions. Fig. 5c illustrates the air is forced to flow into the quarantine room via the door gaps when exhaust fan is operating, which explains the phenomenon of low $SF_{6,conc}$ being detected at the hall-side (i.e., less tracer gas leaked to hall-side), except for the door opening situation.

3.2.3. NV scenarios without exhaust fan

The natural ventilation case without exhaust fan has two fan scenarios: operating with ceiling fan ($NV_{C\text{-}fan}$) and with pedestal fan ($NV_{P\text{-}fan}$). Fig. 3 indicates the NV scenarios took approximately 30 min for the $SF_{6,conc}$ to reach a relatively steady condition (i.e., not a rapid increasing trend), which is faster than at the AC scenarios. The openings from

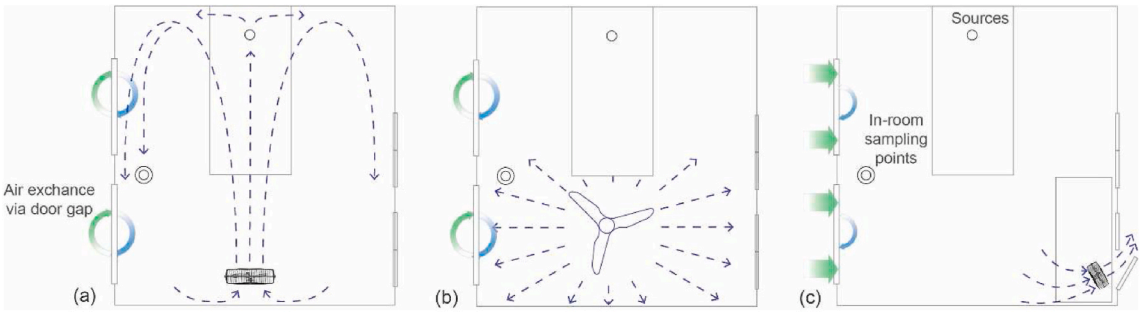

Fig. 5. Plan view of the airflow patterns in air-conditioned scenarios together with the operation of (a) pedestal fan, (b) ceiling fan, and (c) window exhaust fan.

windows and toilet door in NV scenarios enhance air exchange (both infiltration and exfiltration) rate in the quarantine room, leading to lower $SF_{6,conc}$ at equilibrium. Nevertheless, to be consistent with the AC scenarios, we only took the samples from the later 90 min after the door opening procedure as a steady concentration period for our analysis in Fig. 4. The mean (standard deviation) $SF_{6,conc}$ at 0.1 m in-room, 1.7 m in-room, and 0.1 m hall-side are summarized in Table 1.

We found higher in-room $SF_{6,conc}$ in $NV_{C\text{-}fan}$ than in $NV_{P\text{-}fan}$ condition for both sampling heights ($p \leq 0.05$, U test; $|d| \geq 0.474$, large effect size). Meanwhile, our records showed slightly higher $SF_{6,conc}$ at 1.7 m than at 0.1 m in $NV_{C\text{-}fan}$ scenario ($p \leq 0.05$, U test; $|d| = 0.26$, small effect), but the same observation was not found in $NV_{P\text{-}fan}$ case. Plausibly, the airflow pattern generated by the fans led to these differences as the effects of cross ventilation due to outdoor wind is minimal. A plan view in Fig. 6a shows the air (driven by pedestal fan) moves horizontally towards the tracer gas source, then rebound off the walls on both sides. It illustrates a portion of air carrying high $SF_{6,conc}$ could have moved outside the quarantine room through the toilet door and the windows, while a part of the air could have mixed with (or diluted by) the fresh air infiltrating from the toilet, before it is being captured by the in-room samplers. In contrast, the ceiling fan mixes the room air vertically with the recirculated air cells that carries high $SF_{6,conc}$ and moves the air towards the sampler along floor levels before leaving the room (see Fig. 6b). This may explain the reason for higher in-room $SF_{6,conc}$ being detected at $NV_{C\text{-}fan}$ than at $NV_{P\text{-}fan}$ scenario. In addition, stronger airflow at the floor level caused by ceiling leads to a lower $SF_{6,conc}$ at 0.1 m when compared to the sampler at 1.7 m height.

Despite a higher in-room $SF_{6,conc}$ recorded in $NV_{C\text{-}fan}$ scenario, surprisingly a lower $SF_{6,conc}$ was recorded at the hall-side sampler when compared to the $NV_{P\text{-}fan}$ case ($p \leq 0.05$, U test; $|d| = 0.46$, medium effect). We suspect the airflow direction created by the ceiling fan impedes the effectiveness of air exchange via the door gap. Fig. 7a and b, respectively, show a plan view and a side view of air flow through the door gap in $NV_{C\text{-}fan}$ scenario. The ceiling fan moves air which deflects at the floor level, some of which moves horizontally along the floor towards the door, creating a positive pressure gradient between the room and hall along the door gap and forces the room air outwards from one direction (i.e, without fresh air moving in). However, not all air moved by the ceiling fan can get through the door gap. Some of the air hitting the lower part of the door just above the door gap rebounds, creating turbulence which impedes the other air stream movement along the floor towards the door gap (see Fig. 7b).

Compared to the AC scenarios without exhaust, we observed significant reduction in the in-room $SF_{6,conc}$ by 73–80 % (varied by fan types and sampling heights) for the NV scenarios. Similarly, at the hall-side sampler, the $SF_{6,conc}$ has been reduced by 90 % when switching from AC to NV. Apparently, enhanced air change rate inside the quarantine room through window or door openings would effectively reduce tracer gas accumulation, which minimized gas leakage to the hall-side.

3.2.4. *NV scenarios with exhaust fan*

Fig. 4 plots the distribution of steady state $SF_{6,conc}$ for $NV_{C\text{-}fan}$ and $NV_{P\text{-}fan}$ scenarios with window exhaust (denoted by the orange arrow). The mean (standard deviation) $SF_{6,conc}$ at 0.1 m in-room, 1.7 m in-room, and 0.1 m hall-side are summarized in Table 1.

With an operating exhaust fan, our findings show no difference in the $SF_{6,conc}$ between two sampling heights for $NV_{P\text{-}fan}$ scenario ($p > 0.05$, U test), but higher concentration was detected at 1.7 m than at 0.1 m height for $NV_{C\text{-}fan}$ condition ($p \leq 0.05$, U test; $|d| \geq 0.474$, large effect). Meanwhile, we observed the same $SF_{6,conc}$ at 0.1 m height for both fan types ($p > 0.05$, U test). These findings are not much different from the NV scenarios without switching on an exhaust fan, with respect to the airflow patterns illustrated between pedestal and ceiling fan in Fig. 6, thus we expect the same explanations also apply here, moderated by the lower room concentration attributable to the exhaust. We found the in-room $SF_{6,conc}$ reduction rates for NV scenarios (40–45 %) were less than that in the AC scenarios (~80 %) after exhaust fan was turned on. It is likely explained by the air exchange through multiple openings (i.e., toilet door and windows) in NV settings which reduces the effectiveness of exhaust fan operation. Firstly, under NV, the toilet door remains open,

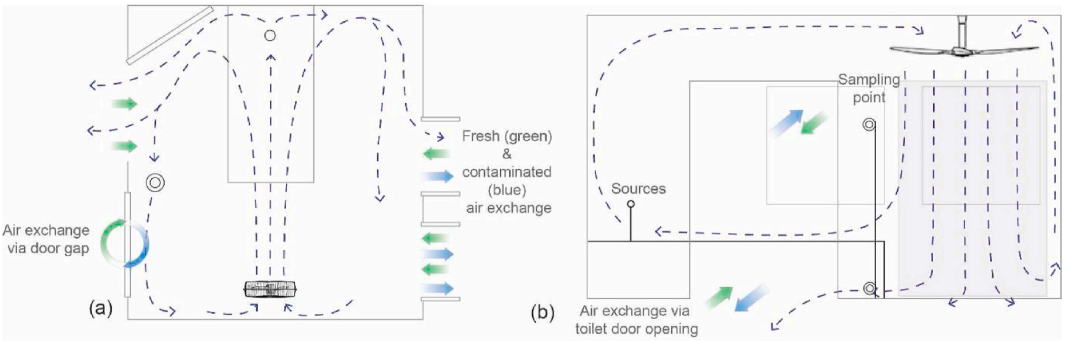

Fig. 6. Schematics of the airflow pattern in naturally ventilated scenarios with windows and toilet door open: (a) plan view operating with pedestal fan, and (b) side view operating with ceiling fan.

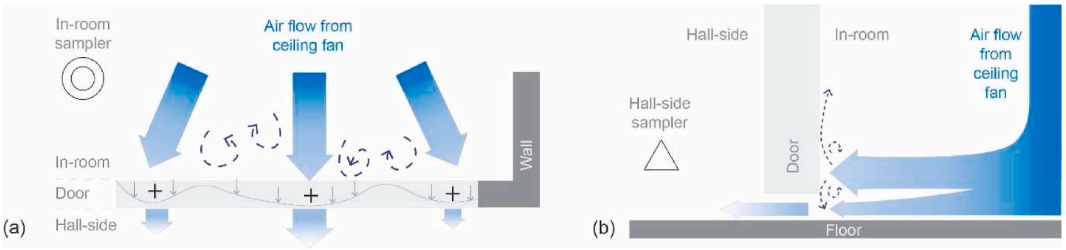

Fig. 7. Illustration diagrams of (a) a plan view and (b) a side vide for airflow generated by ceiling fan passing through the door gap (door between quarantine room and living room). The dotted blue arrows represent the turbulence incurred by the rebound airflow from the door. The grey line and arrows over the door are, respectively, indicating the air pressure gradient and the pressure direction initiated by the fans' airflow. (For interpretation of the references to colour in this figure legend, the reader is referred to the Web version of this article.)

creating an additional volume for the tracer gas to be distributed. Secondly, exhaust fan is exfiltrating the same volume of room air at a lower $SF_{6,conc}$. Nevertheless, the window exhaust is still effective in enhancing the room air change rate (i.e., reducing the in-room $SF_{6,conc}$) in NV conditions. Its contribution towards reducing room concentration is expected to be higher when NV air exchange is limited in low or no wind conditions.

After switching on the exhaust fan, the $SF_{6,conc}$ measured by the hall-side sampler has been reduced by 80 % and 50 %, respectively, for $NV_{P\text{-}fan}$ and $NV_{C\text{-}fan}$ scenarios. Surprisingly, we found higher $SF_{6,conc}$ at the hall-side in NV scenarios, despite a lower steady state in-room $SF_{6,conc}$, when compared to the AC scenarios ($p \leq 0.05$, U test; $|d| \geq 0.474$, large effect). In addition, more tracer gas has been leaked out via the door gap in $NV_{C\text{-}fan}$ than in $NV_{P\text{-}fan}$ case ($p \leq 0.05$, U test; $|d| = 0.3$, small effect). When exhaust fan is operating at AC scenarios, it creates a negative pressure inside the quarantine room and draws air into the room from the only two door gaps, thus the hall-side $SF_{6,conc}$ approaches zero. However, the multiple openings in NV scenarios reduced the "negative pressurization" effect of exhaust fan resulting in a portion of tracer gas still leaking through the door gap due to the airflow mechanism described in Fig. 6. Furthermore, we suspect that the air movement through the door gap in $NV_{C\text{-}fan}$ is dominated by the ceiling fan, pushing air in one direction from the quarantine room towards the hall-side (see Fig. 7a). The exhaust fan can only reduce in-room $SF_{6,conc}$ by increasing air exchange rate through other openings, but unable to compensate for the positive pressure created by ceiling fan at the door gap, resulting in a continuous tracer gas leakage to the living room in the $NV_{C\text{-}fan}$ scenario. Whereas in the $NV_{P\text{-}fan}$ condition, the operating exhaust fan could have maximized the negative pressure via the door gap, meaning that it drives more air into the quarantine room and minimizes air flow outwards to the hall-side. This gives reason for a higher $SF_{6,conc}$ being recorded at hall-side in $NV_{C\text{-}fan}$ than in $NV_{P\text{-}fan}$ scenarios when exhaust fan is switched on.

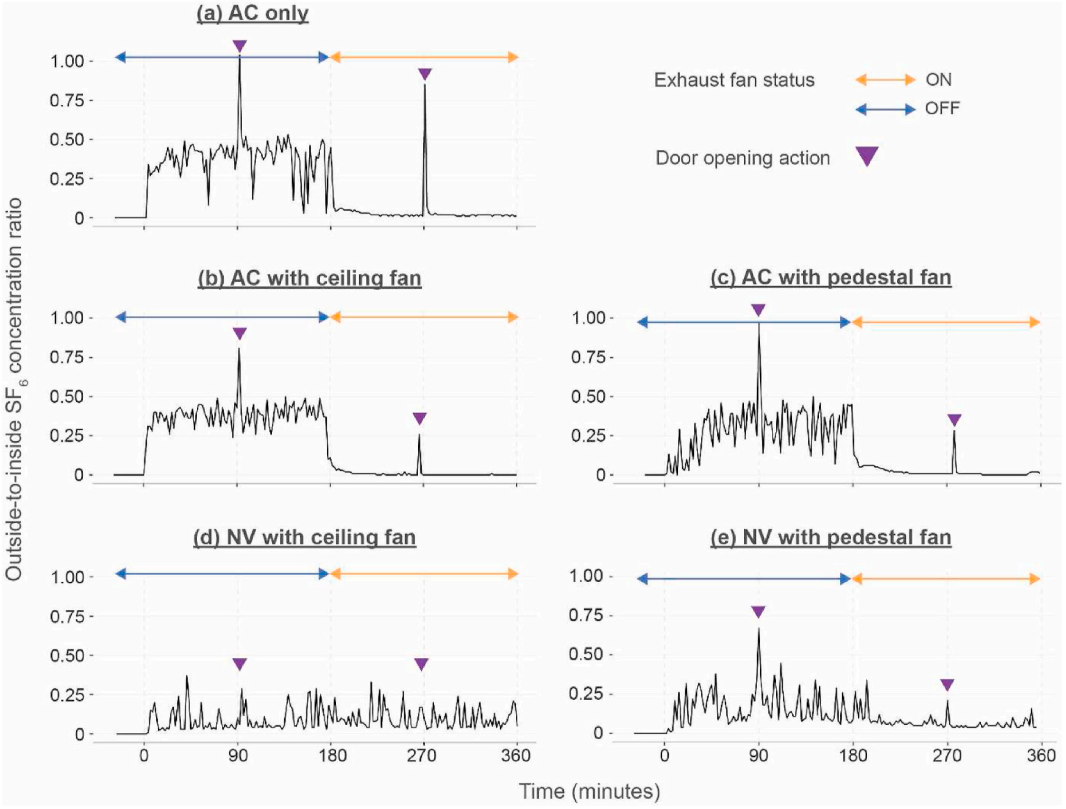

Fig. 8. Time series outside-to-inside (master-bedroom) $SF_{6,conc}$ ratio. (a) AC only, (b) AC with pedestal fan, (c) AC with ceiling fan, (d) NV with pedestal fan, and (e) NV with ceiling fan.

3.3. Outside-to-inside SF_6 concentration ratio

While the absolute $SF_{6,conc}$ values could inform us how high or low the tracer gas level under different scenarios at the three fixed sampling locations, the risk level of tracer gas leakage prior to ventilation effectiveness should have taken both in-room and hall-side $SF_{6,conc}$ into consideration and revealed by the outside-to-inside $SF_{6,conc}$ ratio (O/I_{SF6}). The O/I_{SF6} is calculated by the in-room $SF_{6,conc}$ at 0.1 m over the hall-side $SF_{6,conc}$ at 0.1 m from the same sampling cycle. Time series O/I_{SF6} of the five testing scenarios are plotted in Fig. 8. Observations regarding the door opening action, exhaust fan operation, ventilations, and fan types were discussed in detail below.

3.3.1. Effects of door opening

Although the room door is supposed to be closed all the time during home quarantine, there are some situations when it is opened for a short moment (say around 10 s), such as food delivery and trash clearance. Fig. 8 shows clear spikes of the O/I_{SF6} in all operating scenarios when the door was opened except for the $NV_{C\text{-}fan}$ setting. The rapid increase in O/I_{SF6} is caused by an avalanche of high $SF_{6,conc}$ air flowing out from the quarantine room when the door was opened, with simultaneous hall-side air interchanged with the in-room air, diluting the $SF_{6,conc}$ inside. We observed a higher spike of O/I_{SF6} in AC than in NV scenarios especially for the condition without an exhaust. This is explained by more concentrated tracer gas accumulating inside the AC room without effective ventilation, thus resulting in more rapid gas exchange once the door is opened. In addition, the air density variation driven by temperature difference between in-room (25 °C with air-conditioning) and hall-side (~30 °C common afternoon temperature in Singapore without air-conditioning) air may also enhances air exchange through door opening.

At the door opening moment the O/I_{SF6} was close to 1 in AC_{only} and $AC_{P\text{-}fan}$ scenarios without exhaust fan, meaning that the hall-side $SF_{6,conc}$ was comparable to the in-room $SF_{6,conc}$. It also implies a high risk of infection if someone is at the hall-side, say the one who delivers the food or cleaning up the trash. Interestingly, the spikes of O/I_{SF6} initiated by the opening door were all short, episodic responses without any observable lasting effect, indicating the $SF_{6,conc}$ could have been diffused and settled back to steady quickly at the hall-side. Family members are suggested not staying too close to the quarantine room especially when the door is opened. If necessary, food delivery should be placed at the hall-side before the door is opened or the trash should be cleared sometime after the door has been closed.

Surprisingly, we are unable to see any effect on the O/I_{SF6} due to the door opening for $NV_{C\text{-}fan}$ scenario. We suspect the reasons leading to this observation are two-fold. First, the steady state $SF_{6,conc}$ is relatively low for NV settings with multiple openings. This leads to lower diffusion rate of $SF_{6,conc}$ to the living room even when the door was opened (comparison between $AC_{C\text{-}fan}$ and $NV_{C\text{-}fan}$). We observed a spike in $NV_{P\text{-}fan}$ but not in $NV_{C\text{-}fan}$ scenario. Fig. 6a indicates that the airflow generated by the pedestal fan, moving along the side walls, will directly guide air to move outside the quarantine room when the door is half opened (i.e., at 45° angle). Meanwhile, Fig. 6b shows that, ceiling fan establishes a circulation cell which upward momentum at the door substantially maintained most of the air within the room. The portion that flows along the floor and leaks outwards is somewhat similar, irrespective whether the door was opened or closed. This explains a prompt effect of door opening in O/I_{SF6} found in $NV_{P\text{-}fan}$ but not in $NV_{C\text{-}fan}$ scenario.

3.3.2. Effects of exhaust fan operation

Fig. 8 demonstrates an observable reduction of O/I_{SF6} in all operating scenarios when exhaust fan is switched on except for $NV_{C\text{-}fan}$ setting. More detailed comparison of the O/I_{SF6} is plotted in Fig. 9. The O/I_{SF6} data were selected within the steady state duration (i.e., during 90–180 min when exhaust is turned off and during 270–360 min when exhaust is turned on) consistent with the analysis in former session. The mean (standard deviation) of O/I_{SF6} for exhaust fan [Off: On status] under the five operating scenarios are summarized in Table 2. As mentioned above, we found substantial drop in the O/I_{SF6} after the window exhaust is turned on for all operating scenarios ($p \leq 0.05$, U test; $|d| \geq 0.474$, large effect), except for $NV_{C\text{-}fan}$ ($p = 0.66$, U test; $|d| = 0.05$, negligible effect). It means that operating the exhaust fan not only reduces in-room $SF_{6,conc}$ but effectively minimizes leakage outwards to the hall-side in most of the operating scenarios. The operation of exhaust fan, in $NV_{C\text{-}fan}$ setting, can only reduce in-room $SF_{6,conc}$ (see Fig. 4) but unable to stop the contaminated in-room air from leaking to hall-side due to forced airflow generated by the ceiling fan (explained in Fig. 7).

Table 2
Calculated mean (standard deviation) of the outside-to-inside $SF_{6,conc}$ ratio (O/I_{SF6}) for exhaust fan [Off, On status] at different operating scenarios.

Scenarios	Exhaust fan Off	Exhaust fan On
AC_{only}	0.38 (0.13)	0.02 (0.01)
$AC_{C\text{-}fan}$	0.39 (0.06)	0 (0)
$AC_{P\text{-}fan}$	0.33 (0.12)	0.01 (0.01)
$NV_{C\text{-}fan}$	0.1 (0.08)	0.09 (0.06)
$NV_{P\text{-}fan}$	0.17 (0.10)	0.05 (0.02)

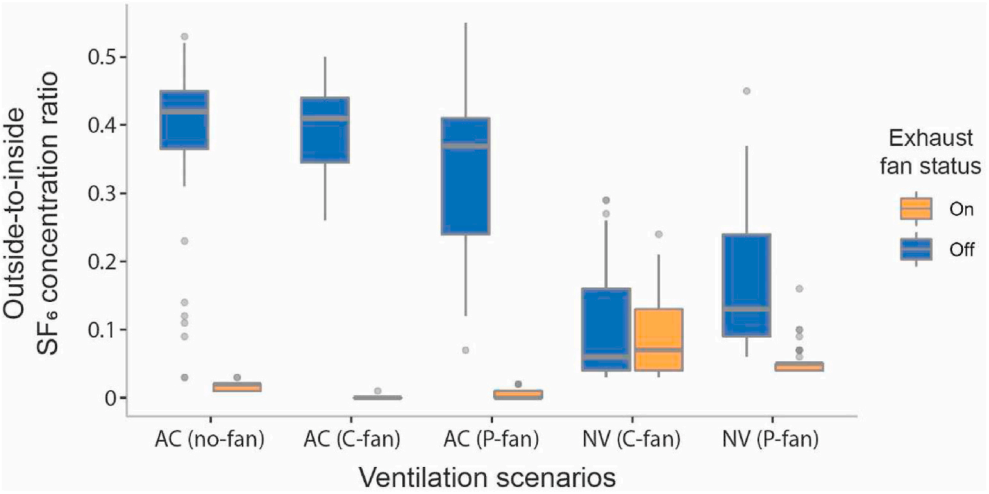

Fig. 9. Boxplot on the steady state outside-to-inside (quarantine room) SF_6 concentration (i.e., O/I_{SF6}) for the conditions with/without window exhaust under five different operating scenarios.

3.3.3. Effects of ventilations and fan types

Without the operation of an exhaust fan, we found a higher O/I_{SF6} in AC than in NV scenarios ($p \leq 0.05$, U test; $|d| \geq 0.474$, large effect). It can be explained by (i) stronger tracer gas diffusion rate to hall-side due to higher in-room $SF_{6,conc}$, and (ii) air density gradient due to in-room (25 °C) and hall-side (~30 °C) temperature deviation. Meanwhile, among the AC settings, we observed lower O/I_{SF6} in $AC_{P\text{-}fan}$ when compared to AC_{only} and $AC_{C\text{-}fan}$ scenarios despite only a small effect ($p \leq 0.05$, U test; $|d| = 0.3$). Considering the $SF_{6,conc}$ leakage to the hall-side was not vastly different among fan types, the observed lower O/I_{SF6} value in $AC_{P\text{-}fan}$ scenario should be contributed by its higher $SF_{6,conc}$ measured inside the quarantine room due to the pedestal fan airflow pattern visualized in Fig. 5a.

After exhaust fan has switched on, Fig. 9 shows higher O/I_{SF6} in NV than in AC scenarios ($p \leq 0.05$, U test; $|d| \geq 0.474$, large effect). We believe the multiple openings available in NV settings reduce the negative pressure effect generated by the exhaust fan across the door gap. In addition, the O/I_{SF6} in $NV_{C\text{-}fan}$ was found higher than in $NV_{P\text{-}fan}$ scenario with window exhaust ($p \leq 0.05$, U test; $|d| = 0.3$, small effect). Considering a similar in-room $SF_{6,conc}$ at 0.1 m found between $NV_{C\text{-}fan}$ and $NV_{P\text{-}fan}$ scenarios in Fig. 4, the difference in O/I_{SF6} value is due to higher tracer gas leakage initiated by the continuous forced air movement from ceiling fan through the door gap (see Fig. 7). This has been discussed briefly in Section 3.2.4.

4. Limitations

The findings in this pilot study have provided us some insight on how to minimize the risk of inter-home virus transmission during home quarantine. However, some limitations are highlighted below before a more holistic study being conducted in the next phase:

- SF_6 tracer is a gas phase particle with ultra-fine particle size. In practice, airborne viruses that are emitted from a patient could be in the form of aerosols over a range of particle sizes. Potential leakage rate or pattern for larger size particles cannot be simulated using only SF_6 tracer. Another emission source with a range of particle size, e.g., olive oil emitted from particle generator, should also be used.
- The instantaneous airflow direction/pattern is likely changing in natural ventilation scenarios. Repeated experiments would have captured slightly different results. We acknowledged this variation and tried our best by avoiding NV scenario experiments in rainy and windy outdoor weather. The wind speeds in Singapore are generally light, with the mean surface wind speed normally less than 2.5 m/s [46,47], and our experiments were conducted during the absence of Northeast Monsoon surge (i.e., when mean wind speeds could be high). In addition, a counter argument is, in real building conditions, we are also unable to assure outdoor airflow patterns, regardless of multiple experimental trials for NV cases in this study. In subsequent studies, we will measure the outdoor environment data using a weather station, to provide information on how the outdoor condition would impact the indoor environment.
- There is a trade-off between the number of sampling points and the sampling frequency when using INNOVA. In this study, we sacrificed multiple sampling points to achieve better sampling frequency for both the in-room and hall-side $SF_{6,conc}$ under different testing scenarios. The drawback is that we are unable to quantify how well the tracer gas is mixed inside the quarantine room. This unknown is especially critical for NV scenarios, whether the air is flowing in from the outdoor to the quarantine room or from quarantine room to the outdoor via the windows. Similarly, with only one sampling point outside the quarantine room, we are unable to quantify whether the tracer gas has been reaching different parts of the house, such as the Living Room where the Sofa is placed, or the Kitchen. Additional equipment or detectors should be introduced with more sampling points distributed inside and outside the quarantine room to check $SF_{6,conc}$ mixing efficiency and mapping the concentration pattern over the entire unit.
- We have sacrificed more sampling points to maximize the sampling frequency (~2 min per sample) from INNOVA, but the duration for door opening activity (~10 s) was still comparatively shorter. It was impracticable to attempt to achieve coincident sampling over the critical (approximately 10 s) door opening duration. The hall-side sampler may or may not be able to capture the highest $SF_{6,conc}$ immediately once the door was opened (i.e., the sampler starts detecting when the tracer gas has been diffused further apart to the living room). Equipment with faster sampling frequency should be used in the upcoming study (i.e., Grimm), which is comparable with the door opening activity.

5. Conclusions

We applied tracer gas technique (SF_6) conducting experiments in a residential like testbed to evaluate the airborne transmission risk through different operating scenarios during home quarantine situations. The tracer gas concentration ($SF_{6,conc}$) in quarantine room and the potential exposure risk for other household members (i.e., the outside-to-inside $SF_{6,conc}$ (O/I_{SF6})) were differed among operating scenarios. We found:

(1) Natural ventilation (NV) reduces concentration levels in quarantine room compared to air-conditioning (AC). The in-room $SF_{6,conc}$ was up to 4 times higher in AC than in NV settings (varied by fan types and sampling height). The opened windows in NV scenarios enhanced the air change rate through cross ventilation inside the quarantine room, which further reduced the amount of trance gas leakage to the hall-side.
(2) The window exhaust fan is effective in reducing exposure of household occupants, and particularly so when air-conditioning is used in the quarantine room. Firstly, the in-room $SF_{6,conc}$ was reduced by 45 % and 80 % when a window exhaust fan was switched on, respectively, for NV and AC scenarios. The reduction in exhaust fan effectiveness was likely attributed to air infiltration from multiple windows or door openings. Secondly, the O/I_{SF6} value dropped significantly in all operating scenarios after operating the exhaust fan, meaning a lower potential risk of airborne transmission, except for the $NV_{C\text{-}fan}$ setting. This finding was explained by the ceiling fan's airflow along the floor level forcing the tracer gas outward from the quarantine room via the door gap.
(3) While both fan types enhanced air mixing inside the quarantine room, the airflow patterns generated from ceiling fan (recirculates air vertically) and pedestal fan (moves air horizontally) were distinct. We believe these airflow patterns contribute to the findings of (i) a difference of $SF_{6,conc}$ between sampling heights when operating ceiling fan and (ii) a clearer observable spike of O/I_{SF6} value after the quarantine room door was opened when operating pedestal fan.

This study provides useful evidence in recommending low risk operating methods for home quarantine situations. However, there are limitations associated with the surrogate particle size, trade-off between sampling points and sampling frequencies, and confounder of cross ventilation in NV scenarios. A more holistic study will be conducted in the next phase to provide more reliable recommendations on operating strategies for home quarantine purpose.

CRediT authorship contribution statement

Toby Cheung: Writing – review & editing, Writing – original draft, Visualization, Methodology, Formal analysis, Data curation, Conceptualization. **Jiayu Li:** Writing – review & editing, Writing – original draft,

Conceptualization. **Jiamin Goh:** Methodology, Data curation, Conceptualization. **Chandra Sekhar:** Writing – review & editing, Supervision, Conceptualization. **David Cheong:** Writing – review & editing, Supervision, Conceptualization. **Kwok Wai Tham:** Writing – review & editing, Supervision, Project administration, Funding acquisition, Conceptualization.

Declaration of competing interest

The authors declare that they have no known competing financial interests or personal relationships that could have appeared to influence the work reported in this paper.

Data availability

The authors have decided not to disclose the data in this pilot study. All data will be shared in the next phase with a more holistic experiment.

Acknowledgment

This research is supported by the National Medical Research Council, Singapore, under its COVID-19 Research Grant (Grant number: COV-ID19RF3-0080). We also thank Dr. Dan Daniel and Ms Wei Yi Wu for their technical assistance.

References

[1] E.G. Bentley, A. Kirby, P. Sharma, A. Kipar, D.F. Mega, C. Bramwell, R. Penrice-Randal, T. Prince, J.C. Brown, J. Zhou, G.R. Screaton, W.S. Barclay, A. Owen, J. A. Hiscox, J.P. Stewart, Sars-CoV-2 Omicron-B.1.1, 529 Variant leads to less severe disease than Pango B and Delta variants strains in a mouse model of severe, COVID-19, (2021) 2021, https://doi.org/10.1101/2021.12.26.474085, 12.26.474085.

[2] E. Callaway, What Omicron's BA.4 and BA.5 variants mean for the pandemic, Nature 606 (2022) 848–849, https://doi.org/10.1038/d41586-022-01730-y.

[3] B. Christie, Covid-19: early studies give hope omicron is milder than other variants, BMJ 375 (2021) n3144, https://doi.org/10.1136/bmj.n3144.

[4] J. Nealon, B.J. Cowling, Omicron severity: milder but not mild, Lancet 399 (2022) 412–413, https://doi.org/10.1016/S0140-6736(22)00056-3.

[5] A. Sigal, Milder disease with Omicron: is it the virus or the pre-existing immunity? Nat. Rev. Immunol. 22 (2022) 69–71, https://doi.org/10.1038/s41577-022-00678-4.

[6] CDC, Quarantine & Isolation, Cent. Dis. Control Prev. (2022). https://www.cdc.gov/coronavirus/2019-ncov/your-health/quarantine-isolation.html. (Accessed 19 July 2022).

[7] Government of the Netherlands, Self-quarantining (Staying at Home) and Coronavirus - Coronavirus COVID-19, 2020 (accessed July 19, 2022), https://www.government.nl/topics/coronavirus-covid-19/tackling-new-coronavirus-in-the-netherlands/self-quarantine/self-quarantaining-or-self-isolating-due-to-coronavirus.

[8] Ministry of Health Singapore, Suitability criteria for home recovery. https://www.covid.gov.sg/HRP-LOU-Suitability-Criteria-for-HRP, 2022. (Accessed 19 July 2022).

[9] K.K. Coleman, D.J.W. Tay, K.S. Tan, S.W.X. Ong, T.S. Than, M.H. Koh, Y.Q. Chin, H. Nasir, T.M. Mak, J.J.H. Chu, D.K. Milton, V.T.K. Chow, P.A. Tambyah, M. Chen, K.W. Tham, Viral load of severe acute respiratory syndrome coronavirus 2 (SARS-CoV-2) in respiratory aerosols emitted by patients with coronavirus disease 2019 (COVID-19) while breathing, talking, and singing, Clin. Infect. Dis. Off. Publ. Infect. Dis. Soc. Am. 74 (2022) 1722–1728, https://doi.org/10.1093/cid/ciab691.

[10] H. Lei, X. Xu, S. Xiao, X. Wu, Y. Shu, Household transmission of COVID-19-a systematic review and meta-analysis, J. Infect. 81 (2020) 979–997, https://doi.org/10.1016/j.jinf.2020.08.033.

[11] S. Chen, Z. Zhang, J. Yang, J. Wang, X. Zhai, T. Bärnighausen, C. Wang, Fangcang shelter hospitals: a novel concept for responding to public health emergencies, Lancet 395 (2020) 1305–1314, https://doi.org/10.1016/S0140-6736(20)30744-3.

[12] J. Ma, No home isolation for China's mild Covid-19 cases, health official says, South China Morning Post. https://www.scmp.com/news/china/science/article/3174044/no-home-isolation-mild-covid-19-cases-chinas-chief, 2022. (Accessed 25 July 2022).

[13] B.V. Duong, P. Larpruenrudee, T. Fang, S.I. Hossain, S.C. Saha, Y. Gu, M.S. Islam, Is the SARS CoV-2 omicron variant deadlier and more transmissible than delta variant? Int. J. Environ. Res. Publ. Health 19 (2022) 4586, https://doi.org/10.3390/ijerph19084586.

[14] F. Rahimi, A. Talebi Bezmin Abadi, Omicron: a highly transmissible SARS-CoV-2 variant, Gene Rep 27 (2022), 101549, https://doi.org/10.1016/j.genrep.2022.101549.

[15] L.A. VanBlargan, J.M. Errico, P.J. Halfmann, S.J. Zost, J.E. Crowe, L.A. Purcell, Y. Kawaoka, D. Corti, D.H. Fremont, M.S. Diamond, An infectious SARS-CoV-2 B.1.1.529 Omicron virus escapes neutralization by therapeutic monoclonal antibodies, Nat. Med. 28 (2022) 490–495, https://doi.org/10.1038/s41591-021-01678-y.

[16] J.W. Tang, A. Nicolle, J. Pantelic, C.A. Klettner, R. Su, P. Kalliomaki, P. Saarinen, H. Koskela, K. Reijula, P. Mustakallio, D.K.W. Cheong, C. Sekhar, K.W. Tham, Different types of door-opening motions as contributing factors to containment failures in hospital isolation rooms, PLoS One 8 (2013), e66663, https://doi.org/10.1371/journal.pone.0066663.

[17] A. Hathway, I. Papakonstantis, A. Bruce-Konuah, W. Brevis, Experimental and modelling investigations of air exchange and infection transfer due to hinged-door motion in office and hospital settings, Int. J. Vent. 14 (2015) 127–140, https://doi.org/10.1080/14733315.2015.11684075.

[18] J.F. San José Alonso, M.A. Sanz-Tejedor, Y. Arroyo, M.R. San José-Gallego, Analysis and assessment of factors affecting air inflow from areas adjacent to operating rooms due to door opening and closing, J. Build. Eng. 49 (2022), 104109, https://doi.org/10.1016/j.jobe.2022.104109.

[19] L. Fontana, A. Quintino, Experimental analysis of the transport of airborne contaminants between adjacent rooms at different pressure due to the door opening, Build. Environ. 81 (2014) 81–91, https://doi.org/10.1016/j.buildenv.2014.05.031.

[20] L. Chang, X. Zhang, S. Wang, J. Gao, Control room contaminant inleakage produced by door opening and closing: dynamic simulation and experiments, Build. Environ. 98 (2016) 11–20, https://doi.org/10.1016/j.buildenv.2015.12.013.

[21] J. Li, M.P. Wan, S. Schiavon, K.W. Tham, S. Zuraimi, J. Xiong, M. Fang, E. Gall, Size-resolved dynamics of indoor and outdoor fluorescent biological aerosol particles in a bedroom: a one-month case study in Singapore, Indoor Air 30 (2020) 942–954, https://doi.org/10.1111/ina.12678.

[22] J. Hou, Y. Sun, Q. Chen, R. Cheng, J. Liu, X. Shen, H. Tan, H. Yin, K. Huang, Y. Gao, X. Dai, L. Zhang, B. Liu, J. Sundell, Air change rates in urban Chinese bedrooms, Indoor Air 29 (2019) 828–839, https://doi.org/10.1111/ina.12582.

[23] World Health Organization, Roadmap to improve and ensure good indoor ventilation in the context of COVID-19 (accessed March 21, 2021), https://www.who.int/publications-detail-redirect/9789240021280, 2021.

[24] Z.T. Ai, A.K. Melikov, Airborne spread of expiratory droplet nuclei between the occupants of indoor environments: a review, Indoor Air 28 (2018) 500–524, https://doi.org/10.1111/ina.12465.

[25] W.L. Oberkampf, T.G. Trucano, Verification and validation in computational fluid dynamics, Prog. Aero. Sci. 38 (2002) 209–272, https://doi.org/10.1016/S0376-0421(02)00005-2.

[26] Q. Chen, J. Srebric, A procedure for verification, validation, and reporting of indoor environment CFD analyses, HVAC R Res. 8 (2002) 201–216.

[27] Z. Ai, C.M. Mak, N. Gao, J. Niu, Tracer gas is a suitable surrogate of exhaled droplet nuclei for studying airborne transmission in the built environment, Build. Simulat. 13 (2020) 489–496, https://doi.org/10.1007/s12273-020-0614-5.

[28] M. Bivolarova, J. Ondráček, A. Melikov, V. Ždímal, A comparison between tracer gas and aerosol particles distribution indoors: the impact of ventilation rate, interaction of airflows, and presence of objects, Indoor Air 27 (2017) 1201–1212, https://doi.org/10.1111/ina.12388.

[29] Z.D. Bolashikov, A.K. Melikov, W. Kierat, Z. Popiołek, M. Brand, Exposure of health care workers and occupants to coughed airborne pathogens in a double-bed hospital patient room with overhead mixing ventilation, HVAC R Res. 18 (2012) 602–615, https://doi.org/10.1080/10789669.2012.682692.

[30] B.C. Singer, H. Zhao, C.V. Preble, W.W. Delp, J. Pantelic, M.D. Sohn, T. W. Kirchstetter, Measured influence of overhead HVAC on exposure to airborne contaminants from simulated speaking in a meeting and a classroom, Indoor Air (2021), https://doi.org/10.1111/ina.12917 ina.12917.

[31] T.L. Gustafson, G.B. Lavely, E.R. Brawner Jr., R.H. Hutcheson Jr., P.F. Wright, W. Schaffner, An outbreak of airborne nosocomial varicella, Pediatrics 70 (1982) 550–556, https://doi.org/10.1542/peds.70.4.550.

[32] S.L. Miller, W.W. Nazaroff, J.L. Jimenez, A. Boerstra, G. Buonanno, S.J. Dancer, J. Kurnitski, L.C. Marr, L. Morawska, C. Noakes, Transmission of SARS-CoV-2 by inhalation of respiratory aerosol in the Skagit Valley Chorale superspreading event, Indoor Air (2020), https://doi.org/10.1111/ina.12751 ina.12751.

[33] S.J. Olsen, H.-L. Chang, T.Y.-Y. Cheung, A.F.-Y. Tang, T.L. Fisk, S.P.-L. Ooi, H.-W. Kuo, D.D.-S. Jiang, K.-T. Chen, J. Lando, others, Transmission of the severe acute respiratory syndrome on aircraft, N. Engl. J. Med. 349 (2003) 2416–2422.

[34] Q. Wang, Z. Lin, J. Niu, G.K.-Y. Choi, J.C.H. Fung, A.K.H. Lau, P. Louie, K.K. M. Leung, J. Huang, P. Cheng, P. Zhao, W. Chen, S. Zhang, L. Fu, P. Chan, A. H. Wong, H. Tse, S.C.Y. Wong, R.W.M. Lai, D.S. Hui, K.-Y. Yuen, D.C. Lung, Y. Li, Spread of SARS-CoV-2 aerosols via two connected drainage stacks in a high-rise housing outbreak of COVID-19, J. Hazard Mater. 430 (2022), 128475, https://doi.org/10.1016/j.jhazmat.2022.128475.

[35] E. Bjørn, P.V. Nielsen, Dispersal of exhaled air and personal exposure in displacement ventilated rooms, Indoor Air 12 (2002) 147–164, https://doi.org/10.1034/j.1600-0668.2002.08126.x.

[36] Y. Li, H. Qian, J. Hang, X. Chen, P. Cheng, H. Ling, S. Wang, P. Liang, J. Li, S. Xiao, J. Wei, L. Liu, B.J. Cowling, M. Kang, Probable airborne transmission of SARS-CoV-2 in a poorly ventilated restaurant, Build. Environ. (2021), 107788, https://doi.org/10.1016/j.buildenv.2021.107788.

[37] National University of Singapore, Smart green homes, NUS News. https://news.nus.edu.sg/smart-green-homes/, 2016. (Accessed 26 July 2022).

[38] K. Mihara, C. Sekhar, Y. Takemasa, B. Lasternas, K.W. Tham, Thermal comfort and energy performance of a dedicated outdoor air system with ceiling fans in hot and humid climate, Energy Build. 203 (2019), 109448, https://doi.org/10.1016/j.enbuild.2019.109448.

[39] A. Field, J. Miles, Z. Field, Discovering Statistics Using R, first ed., SAGE Publications Ltd, 2012. http://gen.lib.rus.ec/book/index.php?md5 = c52094de0c48bfd0d0a232e87c2232df.
[40] E.L. Lehmann, H.J.M. D'Abrera, Nonparametrics: statistical methods based on ranks, Holden-Day, 1975, pp. 5–12.
[41] A. Vargha, H.D. Delaney, A critique and improvement of the CL common language effect size statistics of McGraw and wong, J. Educ. Behav. Stat. 25 (2000) 101–132, https://doi.org/10.3102/10769986025002101.
[42] M. Torchiano, R: Cliff's Delta effect size for ordinal variables. https://search.r-project.org/CRAN/refmans/effsize/html/cliff.delta.html, 2020. (Accessed 26 July 2022).
[43] J. Romano, J.D. Kromrey, J. Coraggio, J. Skowronek, Appropriate statistics for ordinal level data: should we really be using t-test and Cohen'sd for evaluating group differences on the NSSE and other surveys, in: Annu. Meet. Fla., Assoc. Institutional Res., 2006, p. 34.
[44] R. R Core Team, The R Project for statistical computing. https://www.r-project.org/, 2022. (Accessed 26 July 2022).
[45] M. Torchiano, Effsize: efficient effect size computation. https://CRAN.R-project.org/package = effsize, 2020. (Accessed 26 July 2022).
[46] National Environment Agency, Climate of Singapore. http://www.weather.gov.sg/climate-climate-of-singapore/, 2021. (Accessed 25 June 2021).
[47] J. Li, F. Tartarini, Changes in air quality during the COVID-19 lockdown in Singapore and associations with human mobility trends, Aerosol Air Qual. Res. 20 (2020) 1748–1758, https://doi.org/10.4209/aaqr.2020.06.0303.